atmosphere

MDPI

Article

Simultaneous Quantification of Real-World Elemental Contributions from the Exhaust and Non-Exhaust Vehicular Emissions Using Road Dust Enrichment Factor-Elemental Carbon Tracer Method (EFECT)

Duran Karakaş [1,*], Ercan Berberler [1,†], Melike B. Bayramoğlu Karşı [2], Tuğçe Demir [1], Özge Aslan [3,‡], Hatice Karadeniz [3], Ömer Ağa [4,*] and Serpil Yenisoy-Karakaş [5]

[1] Department of Environmental Engineering, Bolu Abant Izzet Baysal University, Bolu 14030, Türkiye
[2] Innovative Food Technologies Development Application and Research Center, Bolu Abant Izzet Baysal University, Bolu 13030, Türkiye
[3] Scientific Industrial and Technological Application and Research Center, Bolu Abant Izzet Baysal University, Bolu 14030, Türkiye
[4] Environmental Engineering Department, College of Engineering, Imam Abdulrahman Bin Faisal University, Dammam P.O. Box 1982, Saudi Arabia
[5] Department of Chemistry, Bolu Abant Izzet Baysal University, Bolu 14030, Türkiye
* Correspondence: dkarakas@ibu.edu.tr (D.K.); oaga@iau.edu.sa (Ö.A.)
† Current address: Department of Environmental Engineering, Bartın University, Bartın 74100, Türkiye.
‡ Current address: Patent Coordination Unit, University of Bakırçay, Izmir 35665, Türkiye.

Abstract: Emission control regulations have been essential in reducing vehicular exhaust emissions. However, the contribution of exhaust and non-exhaust emissions to ambient particulate matter (PM) has not yet been accurately quantified due to the lack of standardized sampling and measurement methods to set regulations. The identified sources and the source profiles generated have not been comparable as none of the emission data collection techniques and the receptor models applied in the literature have produced a standard or reference method to simultaneously identify and quantify the non-exhaust emission sources. This study utilized and thoroughly characterized PM samples including 32 major and trace elements from a mixed fleet in a mountain highway tunnel atmosphere in Bolu, Türkiye. This work proposed a two-stage, simple, and robust method based on road dust enrichment factor (EF) and elemental carbon (EC) tracer methods (EFECT) for the identification and prediction of the exhaust (*exh*), and non-exhaust (*n-exh*) emissions in PM. The indicated method revealed that road dust resuspension emissions are the most significant contributor to the concentrations of crustal elements. This method was used successfully to determine the real-world elemental contributions of road dust resuspension (*rdrs*), emissions (*em*), exhaust (*exh*), and non-exhaust (*n-exh*) emission sources to the elemental concentrations in PM samples. This study provided significant insights into generating actual source profiles, source-specific emission factors, and the source apportionment results for vehicular emission sources worldwide. Considering this, PM data of any particle size fraction (PM_{10}, $PM_{10\text{-}2.5}$, and $PM_{2.5}$, for example) can be used as input for the EFECT, provided that the data include the analytical results of elemental carbon in both the atmospheric PM and road dust samples having similar PM sizes.

Keywords: road dust resuspension; non-exhaust emission; exhaust emission; source apportionment; source profile; EFECT

Citation: Karakaş, D.; Berberler, E.; Bayramoğlu Karşı, M.B.; Demir, T.; Aslan, Ö.; Karadeniz, H.; Ağa, Ö.; Yenisoy-Karakaş, S. Simultaneous Quantification of Real-World Elemental Contributions from the Exhaust and Non-Exhaust Vehicular Emissions Using Road Dust Enrichment Factor-Elemental Carbon Tracer Method (EFECT). *Atmosphere* **2023**, *14*, 631. https://doi.org/10.3390/atmos14040631

Academic Editors: Serena Falasca and Annalisa Di Bernardino

Received: 6 March 2023
Revised: 22 March 2023
Accepted: 24 March 2023
Published: 27 March 2023

1. Introduction

Worldwide and national emission control regulations have played an essential role in reducing vehicular exhaust emissions. In contrast, it is not easy to regulate road dust resuspension and other non-exhaust emissions such as brake, transmissions, hydraulic,

and gear systems of the vehicles, road cover material abrasion, tire wear, and the secondary particles formed in the tunnel atmosphere [1,2]. The existence of a large number of sources emitting particulates with similar compositions to the exhaust emissions hampers the search for useful tracers [3]. The emissions from road dust resuspension and wear processes (brakes, tires, and other moving/rotating parts of the vehicles) are known as non-exhaust sources [4], and it has been stated that even with electric vehicles (EVs), the non-exhaust emissions will still be an essential source of particulate matter (PM) [5,6].

There have been two main types of traffic emission data collection techniques: (1) under controlled conditions and (2) under real-world conditions. As an example of the controlled conditions method, data collection using chassis and engine dynamometer measurements can be considered. However, these tests are not real-world and cannot represent the whole vehicle in a fleet [7]. There are several real-world data collection techniques such as remote sensing, plume chase measurements, portable emissions measurement systems (PEMS), and road tunnel measurements [8–14]. Road tunnel studies involve parallel or concurrent measurements of pollutants at the inlet and the outlet of a bore, or emissions are measured at the mid-point of the bore and the outside of the tunnel for background correction [15,16]. Several receptor models have been used in the literature for source apportionment or source profile generation. Quantitative methods such as the chemical mass balance (CMB) model and multivariate statistical models have been extensively used techniques [8,12,17–20]. However, the CMB model requires well-defined source profiles as inputs. At the same time, positive matrix factorization (PMF) and factor analysis (FA) type techniques may not resolve source contributions effectively when the samples are collected at the source or the vicinity of the emission sources due to the smearing of sources, causing collinearities [21]. For example, Schauer et al. [19] showed that the profiles for gasoline tailpipe and tire wear emissions were collinear, making source separation impossible. Furthermore, multivariate statistical models require a substantial number of PM samples and work efficiently with large datasets. To obtain accurate, representative, and reproducible results from principal component analysis (PCA) type multivariate methods, a minimum variable-to-sample number ratio of 1:3 should be supplied [22]. Therefore, PMF or similar techniques have been used to identify and quantify the source contributions extensively in the literature; however, road dust resuspension and other non-exhaust source emissions, even exhaust emissions, are collinear. Therefore, PMF cannot identify the sources successfully. Because of these source collinearities, the source contributions or apportionment results obtained using PMF or similar techniques (multivariate methods, e.g., principle component analysis, PCA) are not comparable, even in the same region.

Consequently, none of the emission data collection techniques and the tracer or receptor models applied in the literature have produced a standard or reference method to identify and quantify the non-exhaust emission sources simultaneously in real-world conditions. On the other hand, identifying and quantifying traffic-related non-exhaust emissions will always be essential to control and regulate. There has been a great need for a standard method to identify and quantify vehicular emission sources and their contributions. In addition, there has been an ongoing debate in inventory studies due to the inclusion of PM from road dust resuspension causing double-counting [23], which is another problem pending solution.

Considering the above challenges and the needs, this work proposed a two-stage, simple, and robust method to quantify the real-world elemental contributions of vehicular exhaust and non-exhaust emission sources. The advocated new method, abbreviated as the "EFECT" method (Enrichment Factor—Elemental Carbon Tracer), can be applied to a single sample and is not affected by smearing effects from multiple sources. Furthermore, the EFECT will solve double-counting problems in inventory studies.

2. Materials and Methods

2.1. Study Site

Briefly, the study was carried out at the Bolu Mountain Highway Road Tunnel (40.758647° N, 31.446159° E) located on the Transit European Motorway (TEM) line passing through Bolu, Türkiye. Details of the sampling site have been provided in our previous studies [8,10,18] and in Table S1.

Meteorology

The region has a temperate climate, and the long-term (from 1929 to 2021) annual average of wet precipitation is 551.2 mm. Monthly average wet precipitation amounts are 57.7, 48.7, 50.3, 50.6, 60.3, and 58.1 mm for January, February, March, April, May, and June, respectively, while decreasing to 27.8, 24.4, and 28.7 mm, respectively, in July, August, and September. The monthly average wet precipitation amount increased again in October, November, and December to 40.9, 45.1, and 58.7 mm. The long-term (92 years) annual average temperature in the region was 10.4 °C, and it changed from 0.5 °C (January) to 19.9 °C (August) annually. Therefore, the tunnel location is not an arid region and is primarily chilly and foggy, except for July, August, and September.

2.2. Sampling

2.2.1. TSP Sampling

Thermo Andersen GSP II Model PUF (Thermo Anderson Inc., Waltham, MA, USA) were placed on the sidewalk of the south bore, one at the tunnel entrance and the other at the tunnel exit, and the total suspended particulate (TSP) samples were collected on the quartz fiber filters (QFFs, Whatman 110 mm, Merck, Darmstadt, Germany) and pre-fired at 900 °C for 4 h and brought to constant weight in a desiccator before sampling. Concurrent entrance and exit TSP samples were collected at a sampling flow rate of 0.225 m^3/h. Due to high dust loadings on the quartz filters, the sampling time was limited to 1.5–2 h to prevent pressure drops. Laboratory and field blank QFF filters were also prepared and analyzed for the species under consideration. A total of 21 TSP samples were collected during the sampling campaign (23–29 July 2018). The sampling details are given elsewhere [8].

2.2.2. Road Dust Sampling

Road dust samples were collected by manual sweepings from the asphalt surface and sidewalk onto a flat-bottom plastic scoop and then transferred into polyethylene bags. The road dust samples collected at the beginning and end of the sampling campaign were combined before sample preparation for analyses. Samples were passed through a 1.0 mm stainless steel sieve in the laboratory, mixed, and allowed to dry at low temperatures (35–40 °C) in an oven for 24 h. Road dust samples were resuspended under a high-purity nitrogen gas flow (flow rates of 25–35 L/min) in an isolated Plexiglas chamber, and TSP mode particulates were collected on QFFs using one of the PUF samplers that were used for the tunnel TSP sampling. Before starting the PUF sampler for TSP sampling, the nitrogen gas flow was reduced up to a level to have positive pressure in the chamber, and then the sample collection was started. Road dust samples on the QFF filters were subjected to similar analyses as the TSP aerosol samples. This study used stored road dust samples and quartz filters containing TSP samples from the 2018 [8] campaign. For 2019, new road dust samples were collected at the same sampling points.

2.3. Analytical Methods

In this study, 32 major and trace elements (Al, As, B, Ba, Bi, Ca, Cd, Ce, Co, Cr, Cs, Cu, Fe, In, K, La, Mg, Na, Nd, Ni, Pb, Rb, Sb, Sc, Se, Sm, Sr, Th, Tl, U, V, and Zn), water-soluble anions, OC, and EC concentrations in the TSP and road dust samples were determined. QFFs containing TSP samples left from the 2018 sampling campaign were microwave digested (Milestone Start D Microwave Digestion System, Sorisole (BG), Italy) in a concentrated acid mixture of 6 mL nitric acid (Isolab, Eschau, Germany), 1 mL hydrochloric

acid (Merck, Rahway, NJ, USA), and 0.5 mL of hydrofluoric acid (Fluka, Gillman, SA, Australia). Filter samples (TSP and resuspended road dust samples) were digested at 200 °C and 1200 W for 40 min. Element determinations were carried out by using Thermo Scientific X Series Inductively coupled plasma mass spectrometry (ICP-MS) (Waltham, MA, USA). TSP and road dust samples were extracted ultrasonically for 30 min in 50 mL distilled–deionized water and filtered through cellulose acetate filters (0.22 μm). Samples were analyzed for F^-, Cl^-, $NO_2{}^-$, $NO_3{}^-$, $SO_4{}^{2-}$, and $PO_4{}^{3-}$ using the Dionex ICS 1100 model ion chromatography (IC) (Sunnyvale, Canada) with a conductivity detector.

To determine OC and EC in the TSP samples, a desktop OC/EC Analyzer (Sunset Laboratory Inc., Tigard, OR USA) with the NIOSH 870 protocol was used. Details of the sample preparation and analyses for OC and EC are given elsewhere [10].

Most of the anions determined were not included in this study due to having high percentages of negative values in the net concentrations (concentration difference between the concurrent samples of the outlet and inlet stations). All of the data given in this study belonged to the 2018 sampling campaign, except for the road dust samples collected in 2019 and the re-analyses results obtained from the 2018 filter TSP samples. The analytical quality assurance parameters for the analytes are presented in the Supplementary Materials.

2.4. EFECT Method

Briefly, the study followed a two-stage protocol to determine the elemental contributions of road dust resuspension (*rdrs*) and emission (*em*) sources to the particulate matter in a rural tunnel atmosphere. In the first stage of the proposed method, the study estimated the elemental contribution by using the road dust enrichment factor (EF_{rd}). For this purpose, the study used tunnel road dust as the background soil, in contrast to popular crustal or marine enrichment factor applications, and carbonate carbon (CC) in the road dust as the reference element (Table S2). In the second stage, the study used tailpipe EC as a tracer element to estimate the elemental contributions from the exhaust (tailpipe) emissions.

This study used available TSP mode particulate sample data for tunnel aerosol and road dust particulates. The net concentrations of the measured species (X) obtained by subtracting the concurrently measured concentration of X at the inlet station from the outlet station concentration were used to eliminate the contributions from the outdoor atmosphere. The sources of the elements in the tunnel were classified into two categories, namely, *rdrs* and *em*, where the first component involves the resuspension of the previously deposited dust on the road surface. The second component, *em*, on the other hand, consists of the exhaust (*exh*) (tailpipe) and non-exhaust (*n-exh*) emissions. The latter could originate from the vehicle's brake, transmissions, and hydraulic and gear systems. The net concentrations of elements (X) in the TSP samples were denoted as X_{tsp} (or X_{PM10}, $X_{PM10–2.5}$, and $X_{PM2.5}$ for PM_{10}, $PM_{10–2.5}$, and $PM_{2.5}$, respectively, depending on the available PM data), and the concentrations of X contributed by the *rdrs*, *em*, *exh*, and *n-exh* sources were denoted as X_{rdrs}, X_{em}, X_{exh}, and $X_{n\text{-}exh}$, respectively.

Therefore, assuming zero elemental contribution from the outside atmosphere due to the use of net concentration, the X_{tsp} in the tunnel atmosphere can be defined as

$$X_{tsp} = X_{rdrs} + X_{em} \quad (1)$$

where X_{tsp} is the net concentrations of elements in the TSP sample (μg/m^3); X_{rdrs} is the concentration of elements contributed by the road dust resuspension (μg/m^3); X_{em} is the sum of concentrations of elements contributed by the exhaust and non-exhaust emissions (μg/m^3).

Next, the concentration of X contributed by the road dust resuspension emissions (X_{rdrs}) can be determined from Equation (2), as in the case of well-known crustal and marine enrichment factors:

$$X_{rdrs} = \frac{X_{rd}}{CC_{rd}} \times CC_{tsp} \quad (2)$$

where X_{rd} = concentration of X in the reference TSP mode road dust (μg/g); CC_{rd} = concentration of carbonate carbon in the TSP mode road dust (μg/g); the CC_{tsp} = net concentration of carbonate carbon in the TSP aerosol sample (μg/m^3) (Table S2).

In Equation (1), *Xem* represents the fractional concentrations of elements in the TSP samples contributed by the exhaust and the non-exhaust emissions; therefore, X_{em} can be defined as the sum of the exhaust and the non-exhaust emission contributions.

$$X_{em} = X_{exh} + X_{n-exh} \tag{3}$$

In cases where a fleet consists of purely electric vehicles, X_{em} will become equal to $X_{n\text{-}exh,}$ and then X_{rdrs} and $X_{n\text{-}exh}$ can be determined directly from Equations (1) and (2).

In the second stage of the proposed method, the study used the tailpipe (exhaust) EC concentration as a tracer for the exhaust emissions. The study assumed that the elemental carbon (EC) in the rural highway tunnel atmosphere only had two main emission sources: *rdrs* and *exh* emissions. This means that the net concentration of EC (EC_{tsp}) does not have a non-exhaust component, and therefore, EC_{tsp} can be defined as follows:

$$EC_{tsp} = EC_{rdrs} + EC_{em} \tag{4}$$

Then, Equation (3) for the EC becomes

$$EC_{em} = EC_{exh} + 0 \tag{5}$$

Since EC_{em} is equal to EC_{exh}, then the tailpipe EC concentration can be used as a tracer element to estimate the elemental contributions (X) from the exhaust emissions (X_{exh}) (Equation (6)). Finally, the elemental concentrations of X contributed by the non-exhaust sources ($X_{n\text{-}exh}$) can be calculated simply by subtracting X_{exh} from the X_{em} using Equation (7), since $X_{em} \geq X_{exh}$ due to additional non-exhaust source contributions.

$$X_{exh} = \frac{X_{em}^2 \times EC_{tsp}}{X_{tsp} \times EC_{exh}} \tag{6}$$

$$X_{n-exh} = X_{em} - X_{exh} \tag{7}$$

The details of the first (EF) and the second (ECT) stages of the EFECT method and the derivation of Equation (6) are given in the Supplementary Materials.

3. Results

Application Results of EFECT

The study applied EFECT for the source apportionment of the TSP samples corresponding to mixed fleets in the Bolu Mountain Highway Tunnel. The obtained source apportionment results are presented in Table 1 and Table S3, and Figure 1. The results showed that the real-world *rdrs* emission is the most significant contributor to the concentrations of crustal elements such as Mg (66.1%), Ca (63.6%), Mn (62.7%), Al (59.5%), and Fe (44.9%), as expected. The study observed that the *rdrs* emissions were also responsible for about one-third of the TSP concentrations of anthropogenic elements such as Cu (35.7%), V (32.3%), and Zn (38.6%). The regular elemental contribution of *rdrs* to the concentrations of elements related to brake systems such as Sb, Ba, and Sn was observed to be 13.1, 18.2, and 8.0%, respectively.

Table 1. Source apportionment results obtained from EFECT (μg/m^3).

Element	N	X_{tsp}	X_{rdrs}	X_{exh}	$X_{n\text{-}exh}$
Al	14	3.55 ± 0.75 (3.38)	2.11 ± 0.65 (2.53)	0.782 ± 1.03 (0.301)	0.655 ± 0.27 (0.612)
As	18	0.011 ± 0.0073 (0.0103)	0.00113 ± 0.00049 (0.00115)	0.0094 ± 0.0071 (0.0083)	0.00063 ± 0.00032 (0.00063)
Ba	19	0.125 ± 0.0351 (0.117)	0.023 ± 0.010 (0.0231)	0.087 ± 0.041 (0.0753)	0.0140 ± 0.0056 (0.0130)
Be	16	0.00025 ± 5.9×10^{-5} (0.00025)	1.2×10^{-5} ± 5.4×10^{-6} (1.2×10^{-5})	0.00023 ± 6.0×10^{-5} (0.00022)	2.9×10^{-6} ± 2.9×10^{-6} (2.0×10^{-6})
Ca	17	2.84 ± 0.63 (2.72)	1.80 ± 0.76 (1.92)	0.522 ± 0.61 (0.40)	0.509 ± 0.23 (0.537)
Cd	19	0.00054 ± 0.00026 (0.00043)	8.0×10^{-5} ± 3.4×10^{-5} (8.0×10^{-5})	0.00041 ± 0.00026 (0.00033)	5.1×10^{-5} ± 2.0×10^{-5} (5.2×10^{-5})
Cr	19	0.17 ± 0.034 (0.161)	0.0133 ± 0.0058 (0.0135)	0.149 ± 0.038 (0.142)	0.0070 ± 0.0041 (0.0054)
Cu	17	0.041 ± 0.0146 (0.0389)	0.0145 ± 0.0068 (0.0147)	0.0190 ± 0.0170 (0.0152)	0.0072 ± 0.0033 (0.0072)
Fe	15	4.67 ± 3.45 (3.37)	2.10 ± 0.80 (2.38)	1.83 ± 3.82 (0.060)	0.739 ± 0.338 (0.701)
Mg	13	1.07 ± 0.212 (1.05)	0.709 ± 0.226 (0.870)	0.184 ± 0.286 (0.0518)	0.180 ± 0.083 (0.150)
Mn	15	0.045 ± 0.0092 (0.043)	0.028 ± 0.010 (0.0317)	0.0090 ± 0.013 (0.0045)	0.0077 ± 0.0034 (0.0082)
Ni	14	0.044 ± 0.039 (0.0322)	0.0067 ± 0.0031 (0.0066)	0.0331 ± 0.040 (0.0210)	0.0038 ± 0.00166 (0.00406)
Pb	19	0.0196 ± 0.0052 (0.0174)	0.0033 ± 0.0014 (0.0034)	0.0141 ± 0.0056 (0.0120)	0.0022 ± 0.00090 (0.0021)
Sb	19	0.0087 ± 0.002071 (0.00659)	0.00114 ± 0.00049 (0.00116)	0.0069 ± 0.0075 (0.0048)	0.00069 ± 0.00025 (0.00065)
Sn	17	0.0097 ± 0.0095 (0.00663)	0.00078 ± 0.00031 (0.000833)	0.0085 ± 0.0098 (0.0051)	0.00045 ± 0.00023 (0.00049)
V	17	0.018 ± 0.011 (0.0146)	0.0058 ± 0.0026 (0.00620)	0.0091 ± 0.0098 (0.0052)	0.0031 ± 0.0017 (0.00291)
Zn	17	0.168 ± 0.103 (0.155)	0.065 ± 0.028 (0.0689)	0.073 ± 0.11 (0.0565)	0.030 ± 0.0142 (0.0283)
SO_4^{2-}	19	33.2 ± 8.01 (32.7)	3.29 ± 1.47 (3.34)	28.0 ± 8.04 (26.5)	1.95 ± 0.94 (1.80)
OC	18	47.5 ± 13.6 (47.0)	7.70 ± 2.96 (7.49)	34.9 ± 13.5 (36.6)	4.94 ± 1.68 (4.81)
EC	19	42.4 ± 21.0 (40.5)	1.22 ± 0.53 (1.24)	41.2 ± 21.1 (39.2)	0
CC	19	3.23 ± 1.40 (3.28)	3.23 ± 1.40 (3.28)	0	0

Average values ± standard deviations were given with median values in parentheses. N: Number of samples. X_{tsp} (total emission or composite source profile) = X_{rdrs} + X_{exh} + $X_{n\text{-}exh}$. The maximum number of samples was 21. The first two samples were removed from the dataset due to having high outlier results (see Table S1 for the sampling conditions). Any element with N < 19 means that the element has been removed from the corresponding sample due to either negative net concentration (X_{tsp}), negative X_{em} contribution, or negative $X_{n\text{-}exh}$ contribution in the samples.

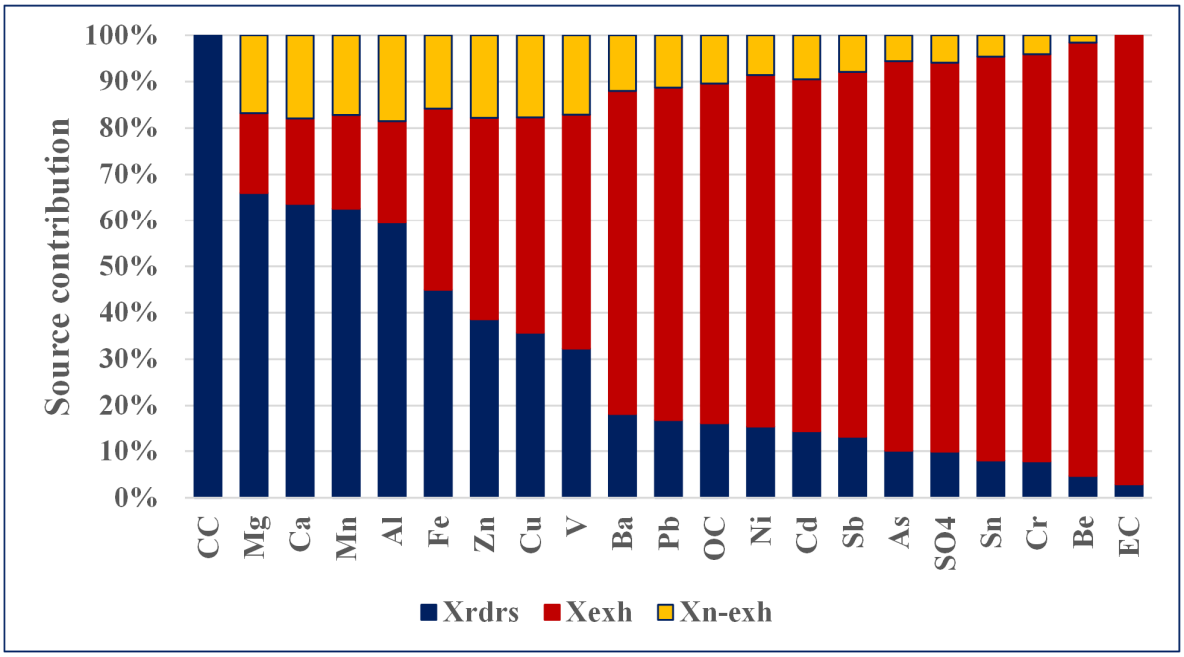

Figure 1. Elemental contributions of *rdrs*, *exh*, and *n-exh* sources on the *tsp* concentrations of elements (%).

The actual *exh* emissions from the mixed fleet were observed to be the most significant contributors of the anthropogenic elements through the combustion processes of fuels, lubricating oils, and wear metals. The EFECT source apportionment results (Table 1, Figure 1) showed that 97.1% of EC, 93.7% of Be, 88.1% of Cr, 87.4% of Sn, 84.2% of SO_4^{2-} and As, 71.8% of Pb, 79.0% of Sb, 76.1% of Cd, 75.9% of Ni, 73.4% of OC, and 69.8% of Ba in the TSP samples were contributed by the *exh* emission sources. Fractional elemental concentrations of V, Cu, and Zn from the *exh* emissions were determined as 50.6, 46.6, and 43.6%, respectively. Except for iron (39.2%), which was 2-fold high, approximately 20% of the *tsp* concentrations of crustal elements (Al, Ca, Mg, and Mn) were observed to be emitted again by the *exh* sources. As discussed in the following sections, exhaust emissions contribute from crustal elements such as Ca and Mg were also reported in the literature. For example, when compared with the values reported for the SPECIEUROPE database, it can be seen that the fractions of Ca and Mg (mass ratios to TSP mass) obtained from the EFECT were almost an order of magnitude smaller than the values reported in the SPECIEUROPE. The fraction of Ca in the exhaust profile was estimated as 0.23 ± 0.23, which was 29.0, 13.0, and 10.0 times lower than the values reported in SPECIEUROPE source profiles, namely, profiles 154, 10, and 140, respectively. Very similar results were also observed for Mg. Mg values estimated from the EFECT was 0.081 ± 0.11 (wt %), which was 6.5, 10, and 2.2 times lower than the values reported in the SPECIEUROPE source profiles. It was reported that diesel and lubricating oils contain elevated concentrations of crustal elements. For example, Smits et al. [24] reported that diesel fuel and lubricating oils have 42 ± 10 ppm and 385 ± 2 0 ppm Ca. They also showed that mass-normalized concentrations of Ca in the undiluted diesel exhaust gas for different load conditions were 0.243 and 0.311 mg/g at 2 and 4 kW loads, respectively. Another study [25] reported that the diesel fuel contained 41,200 µg/L Ca and 7120 µg/L Mg. The concentrations of Ca and Mg in the diesel emissions were reported to be 831 and 138 µg/m^3, respectively. Additionally, the fractions of the Ca and Mg content in the exhaust particles were 28.4% for Ca and 6.2% for Mg at an engine speed of 100%. Weber et al. [26] reported that car motor exhaust emitted significant amounts of Ca, Mg, Si, Fe, Cr, Mn, and Pb. Cheung et al. [27] used gasoline, diesel, and biodiesel cars to estimate the emission factors (EF). They reported that EF for Ca and Mg were determined as 29.7 and 1.59 mg/km for gasoline emissions, 118 and 4.74 mg/km for diesel, and 54.2 and 8.2 mg/km for the biodiesel

emissions, respectively. Furthermore, adding Mg compounds as a detergent dispersant in motor oils can explain the presence of Ca and Mg in the *exh* source profiles. For example, McKenzie et al. [28] reported that exhaust emissions could contain Ca (no value reported) and Mg (6.9 ± 0.2 ppm) due to their presence in motor oils or lubricants. In our previous study [18], for the same tunnel, the study estimated the fraction of Ca and Mg as 36% and 18%, respectively, for diesel exhaust.

In this study, the observed high elemental contributions to TSP concentrations by the exhaust source were due to the positive slope of the tunnel (+2% uphill). This caused more fuel to be pumped, less efficient fuel combustion, and exceptionally high amounts of tracer element (EC) emissions. Therefore, the elemental concentration of EC was the most critical factor in quantifying the *exh* and *n-exh* source contributions.

The non-exhaust emission ($X_{n\text{-}exh}$) source contributions, on the other hand, changed from 1.60 (Be) to 18.5% (Al). Results showed that the *n-exh* sources were responsible for 17.9% of Ca, 17.8% of Zn, 17.7% of Cu, 17.2% of Mn, 17.1% of V, and 16.8% of Mg concentrations in X_{tsp}. Real-world elemental contributions of *n-exh* sources for the Sb, Ni, Cd, OC, Ba, and Fe changed between 7.9 (Sb) and 15.8% (Fe). A group of elements, namely, Cr (4.1%), As (5.6%), Sn (4.6%) including sulfate ion (5.9%) had the lowest contributions from the *n-exh* sources. The EFECT results, in general, showed that the *n-exh* source contributions ($X_{n\text{-}exh}$) were lower than the expected levels that were thought to be due to the positive slope of the tunnel, as discussed above briefly. As the vehicles ascended through the tunnel, the fuel supply increased, which induced poor fuel combustion and higher exhaust emissions (e.g., high OC and EC) as well as lower non-exhaust emissions due to less frequent braking events.

4. Discussion

4.1. Comparison of EFECT's Source Apportionment Results with PMF and FA-MLR

Source apportionment results of EFECT (Figure 1 and Table S3) were compared with the results obtained from well-known receptor models such as positive matrix factorization (PMF) [17,18,29] and factor analysis multiple linear regression (FA-MLR) [8,22]. The authors forced models to run using the same dataset for three sources. The results of the comparison are presented in Table S4. It was observed that both the PMF and FA-MLR methods were unsuccessful in the source identification in this study due to the limited number of samples and the source collinearity [21] between the *rdrs* and *n-exh* source profiles. The effect of this collinearity was observed in the outputs of PMF and FA-MLR, so the sum of X_{rdrs} and $X_{n\text{-}exh}$ was used in the comparisons. The EFECT and PMF provided comparable levels of contributions from the X_{rdrs} + $X_{n\text{-}exh}$ and X_{exh} sources for elements such as Al, As, Fe, Mn, and Zn. However, the sum of the *rdrs* and *n-exh* source contributions obtained from the EFECT for Pb, Sb, Sn, and OC were observed to be 2.0 (OC) to 7.6 (Sn) times lower than the results obtained from the PMF, while the *exh* source contributions for the same elements were 1.9 (OC) to 20.0 (Sn) times lower than the results of the EFECT. Unsatisfactory results were obtained from the FA-MLR (Table S4).

4.2. Road Dust Source Profile Comparisons

Road dust source profiles extracted from SPECIATE, SPECIEUROPE, and the literature [30] were compared with the road dust profile generated in this study. Despite the differences in regional geologies, engine technologies, fuel qualities, and traffic-related infrastructures, the author observed good results for most elements, as shown in Figure 2. Comparisons among the road dust compositions showed that the Cd abundance in our profile was almost an order of magnitude smaller than the result reported in SPECIEUROPE (Profile 12). Again, Ba and Pb abundances were slightly smaller than those reported in other source profiles. On the other hand, the relative amount of sulfate ions in our study was five times and an order of magnitude higher than the abundances reported in the databases and the literature. The organic carbon and EC abundances agreed with most

of the profiles in the table except for the values reported in the SPECIATE source profiles, namely, 3435 and 3425 for OC, and the SPECIEUROPE road dust source profile for the EC.

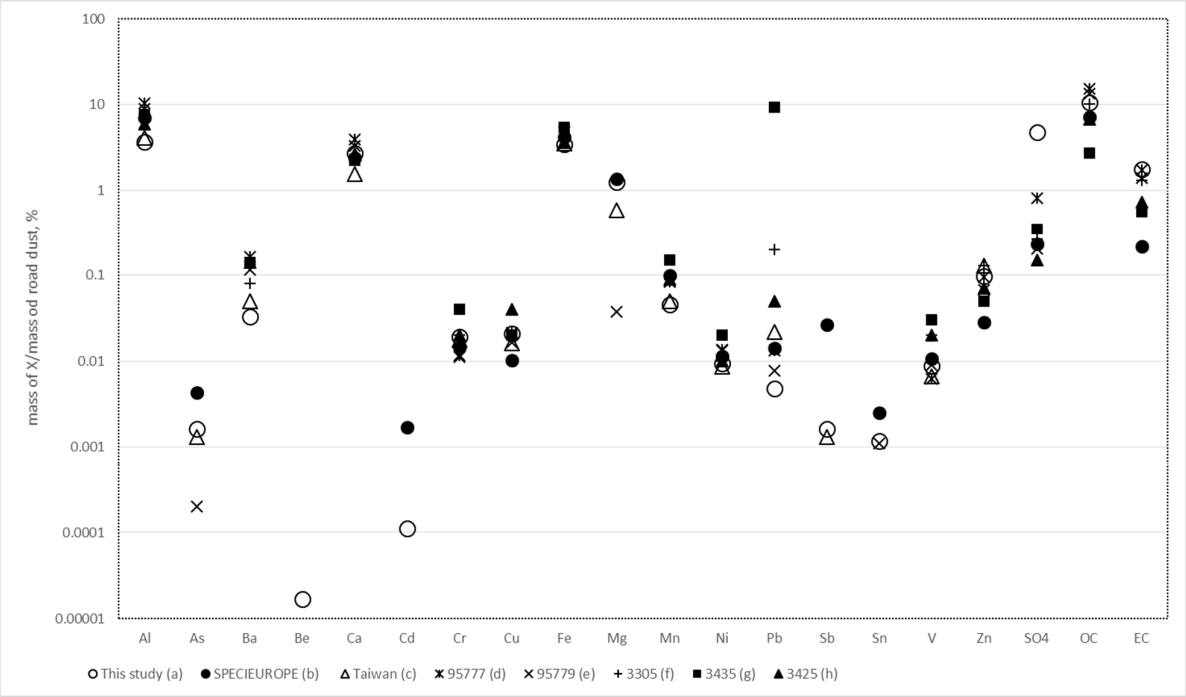

Figure 2. Road dust compositions (masses of elements to mass of road dust ratio, %). (a) Compositions of road dust were determined from the laboratory resuspension (TSP fraction). (b) SPECIEUROPE: Profile no. 12 (Road dust), (c) Wang et al. [30] (Freeway tunnel, SO_4^{2-} was calculated from the reported sulfur concentration), (d) SPECIATE: Profile no. 95777 (Paved road dust, PM_{10}).

4.3. Exhaust Emission Source Profile Comparisons

This study compared the *exh* source profile generated with the available exhaust source profiles in the SPECIEUROPE and SPECIATE databases. The exhaust source profiles in the databases have been reported as mass ratios; therefore, for comparison purposes, the study normalized the source apportionment results of the EFECT with the *TSP* mass of the corresponding samples. Comparison results of the exhaust source profiles obtained from the EFECT with the reported profiles in SPECIEUROPE (Table S5 and/or Figure S2) and SPECIATE (Table S6) showed, even though the comparison of the source profiles was not very meaningful due to the reasons above-mentioned, reasonable agreements. Using source profiles extracted from the SPECIATE and SPECIEUROPE databases and/or the literature in inventory studies may cause severe uncertainties in the results due to known regional differences in geological materials and other essential factors such as engine technologies in the fleets, fuel qualities, fleet compositions, and the meteorological conditions during the sampling campaigns. Therefore, specific source profiles representing a specific region have to be generated. For example, the source profiles generated in this study correspond to the western Black Sea region of Türkiye and may not represent the more arid regions such as the central and eastern regions of the country. The average fleet composition in Türkiye, as of 2019, was 38% diesel-fueled, 38% LPG-fueled, and 24% gasoline-fueled passenger cars [8]. At the same time, the average fleet compositions in the Bolu Mountain Highway Tunnel involved approximately 67% diesel-fueled and 33% LPG and gasoline-fueled vehicles [8]. When the average fleet composition, geology, climate, and the uphill slope (+2%) in this study were considered, different real-world source profiles must have been expected for other regions.

High standard deviations observed in the source profiles of EFECT were because the samples were collected at different times (morning, noon, and afternoon), and the

corresponding changes took place in the fleet compositions during sampling. Therefore, the standard error of the mean can be used as uncertainty for an element in a profile to define a confidence interval in which the population means are most likely to fall.

Comparison results showed that the percent abundances of Ca, Cd, Cu, Fe, Mg, Mn, Pb, Sb, Sn, and Zn in the *exh* component of EFECT were smaller than the values reported in the SPECIEUROPE source profiles. At the same time, the rest of the elements showed agreement with the results reported in the database. It should be emphasized again that in the comparison results, the sample PM size, fleet composition, regional geology, and climate should be considered as the main factors responsible for the variances in the regional source profiles.

The comparison of the *exh* source profiles obtained from EFECT and SPECIATE is presented in Table S6. It should be noted that the *exh* source profiles reported in SPECIATE corresponded to the $PM_{2.5–10}$, PM_{10}, and PM_{30} samples from transportation in the Sepulveda Tunnel (Los Angeles). Although the source profile generation was conducted in 2004, and the SPECIATE source profiles were generated from the data collected more than three decades ago, therefore, the emission rates are expected to have changed with the significant improvements in engine technologies, fuel qualities, and other transportation infrastructures. As a result of these improvements, it was observed that the mass percentage of Pb in the EFECT's *exh* source profile was 70 to 140 times lower than the Pb abundances in the SPECIATE's exhaust source profiles. Similar outcomes of these improvements were also observed for Zn (1.6 to 3.6 times), OC (2.6 to 4.0 times), and EC (1.0 to 3 times) in our results. In this study, the *exh* contribution to the sulfate fraction was very high compared to the values reported in the SPECIEUROPE source profiles. There is a specific factor that should be discussed for the observed sulfate fraction from the *exh*. In Türkiye, it is well-known that there has been extensive use of non-standard diesel fuels produced illegally by blending used or waste engine oils with standard diesel fuels and sold for trucks, semi-trailer trucks, and coaches. EPDK (Energy Market Regulatory Authority, Republic of Türkiye) reports that engine oil blended non-standard diesel fuels are ubiquitous in the petroleum market due to their low prices. This fuel is known as "Number 10 Engine oil" in the market in Turkiye. Since the viscosity of number 10 engine oil is not similar to standard diesel, the fuel is sprayed into the combustion chamber without being atomized, and complete combustion does not occur. In this case, engine performance decreases, and emissions increase. A study reported that the composition of the ship-engine heavy fuel oil PM was dominated by organic matter, black carbon, and sulfates, and the dominant sulfate species was sulfuric acid [31]. Unfortunately, there are no research data on the engine oil-blended diesel fuel emissions for Türkiye. However, this study's high exhaust sulfate is expected to be due to the use of engine oil-blended diesel fuels in Türkiye, even though such practices have been prohibited.

4.4. Diagnostic Ratios for rdrs, exh, and n-exh Sources

The most widely used diagnostic ratios for the *rdrs*, *exh*, and *n-exh* sources from the source apportionment results of the EFECT are presented in Table S7. The most frequently reported diagnostic ratios in the literature are Fe, Ba, Sb, Sn to Cu, and OC to EC ratios [29,32–36]. The calculated diagnostic ratios were compared with the literature values reported mostly for PM_{10}, coarse PMs ($PM_{10–2.5}$), and $PM_{1.8\text{-}10}$ due to the limited number of reported ratios for TSP. It was observed that the diagnostic percentages reported in the literature [7,29,32–34,36–38] mostly agreed with the ratios obtained from X_{tsp} and X_{exh}.

The mean Sb/Cu ratios in the X_{rdrs} and $X_{n\text{-}exh}$ components were calculated as 0.078 and 0.076 $\pm$ 0.014, respectively, which were not different from each other statistically. As in the case of the Sb/Cu ratio, the Sn/Cu ratios were also observed to be similar for both X_{rdrs} and $X_{n\text{-}exh}$ as 0.056 and 0.064 $\pm$ 0.0092, respectively, Therefore, it is clear that the diagnostic ratios of Ba, Sb, and Sn to Cu in X_{rdrs} were almost similar to their corresponding percentages in the $X_{n\text{-}exh}$. When the source apportionment results obtained from the EFECT were examined, it was observed that their percent elemental contributions were in the

range of 18.0–21.0% in X_{rdrs}, 66.0–71.0% in X_{exh}, and 11.0–13.0% in $X_{n\text{-}exh}$. Therefore, the similar behavior of these three elements indicated that they had common sources. The linear relationship between the TSP concentrations of Fe, Cu, Sb, and Sn ($0.80 < R2 > 0.94$) also confirmed that they mainly came from similar sources [7,29,37]. The diagnostic ratios determined for the *rdrs* and *n-exh* sources showed that these two sources were collinear when their standard deviations and ranges were considered. In this case, it was almost impossible to discriminate between these two sources using the multivariate receptor models, as also observed during the EFECT, PMF, FA-MLR comparisons. The authors believe that the ratios provided in the generated source profiles from the EFECT would be a more suitable solution for more comparable and representative diagnostic ratios.

The *tsp* and the fractional concentrations of Ba contributed by *rdrs*, *n-exh*, and the *exh* emissions should be evaluated separately. Since barium sulfate ($BaSO_4$) is the primary filling material in brake lining, measured concentrations of Ba in PM samples at a traffic site have generally been attributed to brake wear [8,13,36,39]. However, barium sulfate is an acid-insoluble salt and may not be entirely recovered from the particulate matter (PM) samples if the samples are acid digested. Unless nuclear analytical techniques [9] or the alkali fusion method [40] are used, the exact amount of Ba in the samples cannot be recovered. This study's high percentage of Ba observed in the exh component relative to rdrs and n-exh sources supports our claim for Ba recovery from the traffic-site PM samples. Consequently, the authors believe that the Ba concentrations measured in the roadside PM and road dust samples mainly came from acid-soluble compounds such as organometallic barium (e.g., barium-containing additives for soot suppression [41] and inorganic Ba compounds (carbonate, nitrate, and chloride salts of barium) originating from vehicular exhaust emissions, road surface paintings [8,18], and local crustal soils rather than $BaSO_4$ from the brake lining. In conclusion, the observed results in this study suggest that barium cannot be a suitable marker element for brake wear processes due to having too many sources, even though a detectable amount of Ba comes from the barium sulfate, which was detected in the study as brake wear emission.

4.5. Source Profiles Generated from the EFECT

Using the *tsp* mass to normalize source contributions from the EFECT caused similarities or decreases in the code of divergence (COD) [38] between the source profiles. To increase the divergence between the source profiles, this study normalized the source contributions with their source markers, namely, the net TSP concentration of carbonate carbon (CC_{tsp}), EC_{exh}, and $Cu_{n\text{-}exh}$ for the *rdrs*, *exh*, and *n-exh* sources, respectively (Table 2). The source profiles generated by normalizing the sources with their marker elements increased the coefficient of divergence between the source profiles of the *rdrs* and *n-exh* sources 2.1 times (from 0.478 to 0.990). In contrast, the COD between the source profiles of the *rdrs* and *exh* sources increased slightly from 0.583 to 0.627. The lowest COD value was observed for the *tsp* (total or composite emission) and the *exh* source profiles (COD = 0.529), which were expected, since the *exh* emission was the main contributor of the elements measured in the TSP samples through fuel combustion. The COD between the *exh* and *n-exh* source profiles changed significantly from 0.635 to 0.996. Therefore, it is clear that the generated source profiles given in Table 2 are almost entirely different. Consequently, the source profiles generated from the results of the EFECT can be used as inputs in chemical mass balance type receptor models. These can be applied directly to the receptor sites as vehicular source profiles to quantify the *rdrs*, *exh*, and *n-exh* source contributions.

Table 2. Source profiles of the *rdrs*, *exh*, and *n-exh* vehicular sources for a mixed fleet (mass of X to mass of corresponding marker element ratios).

		rdrs	***exh***	***n-exh***
	N	**Mean ± Std**	**Mean ± SE**	**Mean ± SE**
Al	14	0.783 ± 0.058	0.032 ± 0.0056	119.4 ± 12.0
As	17	$0.00035 \pm 2.5 \times 10^{-5}$	$0.000333 \pm 3.8 \times 10^{-5}$	0.0759 ± 0.0059
Ba	17	0.00704 ± 0.00085	0.00240 ± 0.00021	1.61 ± 0.029
Be	15	$3.63 \times 10^{-6} \pm 5.8 \times 10^{-7}$	$6.98 \times 10^{-6} \pm 3.1 \times 10^{-7}$	$0.00040 \pm 3.1 \times 10^{-5}$
Ca	16	0.586 ± 0.046	0.0207 ± 0.0035	97.0 ± 5.11
Cd	17	$2.42 \times 10^{-5} \pm 1.6 \times 10^{-6}$	$9.34 \times 10^{-6} \pm 2.2 \times 10^{-6}$	0.00582 ± 0.00025
Cr	17	0.00411 ± 0.0011	0.00337 ± 0.00028	0.940 ± 0.077
Cu	15	0.00452 ± 0.00045	$0.000575 \pm 5.3 \times 10^{-5}$	1.00 ± 0.00
Fe	14	0.736 ± 0.059	0.0245 ± 0.0055	115.0 ± 9.11
Mg	13	0.267 ± 0.026	0.00738 ± 0.0011	45.7 ± 2.56
Mn	15	0.00971 ± 0.00069	$0.00275 \pm 4.9 \times 10^{-5}$	1.580 ± 0.14
Ni	13	0.00201 ± 0.00022	0.000883 ± 0.00016	0.456 ± 0.015
Pb	17	$0.00102 \pm 6.6 \times 10^{-5}$	$0.000338 \pm 2.5 \times 10^{-5}$	0.240 ± 0.0064
Sb	17	$0.000352 \pm 2.8 \times 10^{-5}$	$0.000145 \pm 7.6 \times 10^{-5}$	0.0760 ± 0.0044
Sn	16	$0.000254 \pm 1.8 \times 10^{-5}$	$0.000155 \pm 1.3 \times 10^{-5}$	0.117 ± 0.063
V	15	0.00190 ± 0.00015	$0.000165 \pm 2.5 \times 10^{-5}$	0.390 ± 0.026
Zn	16	0.0210 ± 0.0014	0.00170 ± 0.00020	4.14 ± 0.21
SO_4^{2-}	17	1.020 ± 0.096	0.914 ± 0.100	228.0 ± 6.71
OC	16	2.280 ± 0.222	1.41 ± 0.120	564.0 ± 25.5
EC	17	0.380 ± 0.180	1.00	0.00

X_{rdrs}, X_{exh}, and $X_{n\text{-}exh}$ concentrations obtained from the source apportionment results of EFECT were normalized with CC_{tsp}, EC_{exh}, and $Cu_{n\text{-}exh}$, respectively. Results were reported as the mean ± standard deviation (Std) for the *rdrs* and mean ± standard error (SE) for *exh* and *n-exh*. Results for the first three samples were not included in this table due to having high outliers for all of the measured elements (see Table S1 for sampling conditions). Additional outliers (high and low) in the dataset were removed by applying the Q-test before calculating the reported means and the uncertainties. N shows the number of samples used to calculate the means of each element and can be used to convert the standard deviation into the standard error (SE) for the *rdrs* source profile.

4.6. Receptor Site Application Results of the EFECT

To show the field applicability of the EFECT source profiles given in Table 2, the model was applied at another receptor site, namely, the Gölcük Nature Park in Bolu (Türkiye), which is frequently under the influence of intense barbecue smoke and an uncontrolled number of visitors [42]. Application of the *rdrs* and *exh* source profiles showed that 16.0 ± 6.24% of OC and 29.5 ± 7.11% of EC were contributed by the road dust resuspensions created by the vehicles and the visitors at the parking area and the sampling point, and 13.1 ± 4.35% of OC was contributed by the vehicular *exh* emissions at the vicinity of the Nature Park (Table S8). Results obtained from the receptor site showed that the *rdrs* and the *exh* source profiles generated from the EFECT can be used as in the case of well-known crustal enrichment factor calculations.

4.7. Using Source Apportionment Results of the EFECT as Inputs to PMF

Identifying and quantifying the sources by the EFECT create new sub-datasets free from the negative effects of the source collinearities in the source identifications. Since the PMF and other multivariate source apportionment techniques are receptor oriented, they become insufficient in source identification applications when the samples are collected at the sources, as discussed in the introduction. Fortunately, the study observed that the EFECT eliminates the source collinearities by identifying the three primary emission sources: *rdrs*, *exh*, and *n-exh*. Therefore, the new sub-datasets can be used as inputs for a receptor model like PMF to further identify the common sources comprising the three main sources. The source apportionment results of EFECT (used to create Table 1) were used as inputs for the PMF, and more promising results were obtained.

When the *rdrs* results were used as the input, the study successfully identified the local soil and the traffic-related dust sub-sources. It quantified their relative elemental

contributions to the total *rdrs* emissions. The PMF output results showed that 3.8% to 4.20% of all the anthropogenic elements originated from the local soil, interestingly including iron, which is a well-known crustal element while 60.0, 63.2, 66.7, 67.1, and 67.4% of Be, Ca, Mg, Mn, and Al, respectively, were observed to be contributed by the local soil [8,19].

Using the *exh* component of the EFECT source apportionment result as input for the PMF identified diesel and gasoline-LPG emissions and quantified their partial elemental contributions. Results showed that 99.5, 73.4, 70.6, 69.4, 67.1, 56.8, and 50.3% of As, SO_4^{2-}, EC, Pb, Be, Ba, and diesel emissions contributed OC. On the other hand, 100.0, 90.8, 80.1, 72.6, 49.7, 30.6, and 29.4% of Ni, Cu, Sb, Sn, OC, Pb, and EC, respectively, were observed to be contributed by gasoline-LPG fuel combustion emissions. The study discriminated the diesel and the gasoline-LPG emissions from their EC and OC levels. Unlike diesel emissions, gasoline-LPG-fueled vehicles emit more OC than EC [18,43]. For the *exh* dataset, the study ran the PMF for two factors, neglecting the secondary particle formation of sulfates. However, running the PMF for at least three factors would be better to identify additional sources together with the diesel and gasoline emissions.

When the sub-dataset obtained from the EFECT for the *n-exh* emissions was used as the input, PMF identified three sources: (1) brake and tire wear with high loadings of brake wear marker elements and tire wear [19,38,44–46]; (2) road cover material abrasion, which was characterized by high and moderate loadings of crustal elements and OC, respectively [8]; (3) vehicular hydraulic and gear systems, bearings, and coils which were characterized with the contents of wear metals such as Ni, Cu, Fe, Mn, Al, and Cr [19,47]. According to the PMF results, the first source contributed mainly to concentrations of Zn (79.6%), Sn (68.0%), Sb (57.6%), Cr (57.6%), Ba (47.8%), Pb (46.7%), Cd (46.9%), SO_4^{2-} (43.4%), Cu (31.5%), and Ni (22.1%). The second *n-exh* source, road cover material abrasion, was observed to be responsible for 83.7% of Al, 74.7% of Mn, 70.6% of Mg, 68.3% of Fe, and 20.7 to 33.6% of OC, Ba, Cd, Pb, As, SO_4^{2-}, and Cr in the total elemental concentrations originating from the non-exhaust emissions. High relative elemental contributions were observed for Ni (77.9%) and Cu (68.4%). Comparatively, lower contributions were observed for Fe (31.7%), OC (29.8), and 29.0 to 29.6% of SO_4^{2-}, Ba, Pb, and Cd, 25.5% of Sb, 25.3% of Mn, 16.6% of Sn, 12.8% of Zn, 12.6% of Al, 8.9% of Cr were attributed to the third non-exhaust emission source [47].

5. Conclusions

There has been a scarcity of real-world *n-exh* and *rdrs* source profiles studies, which is an important problem in receptor modeling since the identified sources and the source profiles generated through these studies have not been comparable. Considering these challenges, this study showed that the EFECT model could be a primary standard method to fill these important gaps in the literature, especially in quantifying source contributions, generating real-world source profiles, and source-specific emission factors for the vehicular *rdrs*, *exh*, and *n-exh* emission sources. In the literature, generally, the empirical equation developed under USEPA AP-42 emission factors has been used worldwide [48] for the estimation of PM contribution from road dust resuspension. However, different equations and constant input variables have been used for paved and unpaved roads and the formulations, respectively [49–55], making the method more complex and challenging in applications. The current proposed EFECT method identifies and quantifies *rdrs* contribution independently from factors such as road cover materials and vehicle types. Relative source contributions from the EFECT were more practical than those obtained from receptor-oriented techniques such as PMF and FA-MLR. The study observed acceptable agreements among the source profiles reported in SPECIATE, SPECIEUROPE, and those generated from the EFECT. It was observed that the main contributor of the anthropogenic elements was exhaust emissions, followed by road dust resuspension emissions. This study revealed that road dust resuspension emissions are the most significant contributor to the concentrations of crustal elements such as Mg (66.1%), Ca (63.6%), Mn (62.7%), Al (59.5%), and Fe (44.9%), while there was 97.1% of EC, 93.7% of Be, 88.1% of Cr, 87.4% of Sn, 84.2% of

SO_4^{2-} and As, 71.8% of Pb, 79.0% of Sb, 76.1% of Cd, 75.9% of Ni, 73.4% of OC, and 69.8% of Ba in the PM samples. On the other hand, the contribution by exhaust emission sources and non-exhaust emission source contributions changed from 1.60 (Be) to 18.5% (Al).

This study also showed that the EFECT method could apply to receptor sites and its source apportionment results can be used as inputs for receptor models for the further identification of additional specific emission sources such as local soil, traffic-related dust, road cover material abrasion, brake and tire wear, diesel and gasoline-LPG, and the transmission and gear systems of vehicles. In conclusion, the study assumes that the EFECT method is a simple model that will revolutionize traffic-based pollutant source apportionments, source profiles, and emission factor generations. One of the most significant achievements is that it can effectively discriminate contributions from road dust resuspension and other non-exhaust emissions.

Supplementary Materials: The following supporting information can be downloaded at: https://www.mdpi.com/article/10.3390/atmos14040631/s1, Table S1: Sampling descriptions, the Bolu Mountain Highway Tunnel Study (23 July through 29 July 2018); Table S2: Mean concentrations of elements in the tunnel road dust samples collected in 2018 and 2019 (μg X/g road dust) and means of the road dust elemental concentration ratios to the road dust CC concentrations; Table S3: Relative real-world elemental contributions of vehicular sources (%); Table S4: Comparison of the relative elemental contribution results of EFECT with PMF and FA-MLR (%); Table S5: Real-world source profiles (mass of element to tsp mass) for a mixed fleet obtained from the EFECT method and comparison with the SPECIEUROPE source profiles (%); Table S6: Comparison of the *exh* source profiles obtained from the EFECT and SPECIATE database; Table S7: Diagnostic ratios of the selected elements for the vehicular emission sources; Table S8: Road dust resuspension (*rdrs*) and *exh* source contributions on the TSP size and OC and EC concentrations at the receptor site; Table S9: Method detection and quantification limits (MDL and MQL) and the percent recoveries of the elements and sulfate ions. Figure S1: Mean road dust enrichment factors of the elements in the tunnel atmosphere relative to TSP fraction of the tunnel road dust; Figure S2: Real-world *exh* source profiles (mass of element to tsp mass) for a mixed fleet obtained from the EFECT method and a comparison with the SPECIEUROPE source profiles (%); File S1: The first stage of the EFECT: Road dust enrichment factors, EF_{rd} (EF); File S2: The second stage of EFECT: Exhaust EC tracer method (ECT).

Author Contributions: D.K.: Conceptualization, methodology, writing—original draft preparation, writing—review and editing, and supervision; E.B., M.B.B.K., T.D., and Ö.A. (Özge Aslan): Field sampling, sample analyses, data gathering; H.K.: Conducted the PMF and interpreted the results; Ö.A. (Ömer Ağa): Resources, writing—review and editing; S.Y.-K.: Participated in field sampling, proposed carbonate carbon as a reference element for the road dust, and edited the manuscript. All authors have read and agreed to the published version of the manuscript.

Funding: This research was partially funded by Abant Izzet Baysal University, Scientific Project Unit with grant no: 2017.33.01.1231.

Data Availability Statement: The data used for this study are held by the authors. Please contact the corresponding author (D.K.) for details.

Acknowledgments: The authors acknowledge Arzu Kurt and Murat Kara (Bolu Abant Izzet Baysal University) for their support in the derivations of the equations, Murat Kiliç (Akdeniz University) for their contribution to the elemental analyses, Beyhan Pekey for supplying the PUF sampler, and Rosa Flores (Marmara University) for making the OC/EC analyzer available for us to carry out the cross-check analyses of the road dust samples.

Conflicts of Interest: The authors declare no conflict of interest.

References

1. Amato, F.; Cassee, F.R.; Denier van der Gon, H.A.C.; Gehrig, R.; Gustafsson, M.; Hafner, W.; Harrison, R.M.; Jozwicka, M.; Kelly, F.J.; Moreno, T.; et al. Urban air quality: The challenge of traffic nonexhaust emissions. *J. Hazard. Mater.* **2014**, *275*, 31–36. [CrossRef] [PubMed]
2. Denier van der Gon, H.A.C.; Gerlofs-Nijland, M.E.; Gehrig, R.; Gustafsson, M.; Janssen, N.; Harrison, R.M.; Hulskotte, J.; Johansson, C.; Jozwicka, M.; Keuken, M.; et al. The Policy Relevance of Wear Emissions from Road Transport, Now and in the Future-An International Workshop Report and Consensus Statement. *J. Air Waste Manag. Assoc.* **2013**, *63*, 136–149. [CrossRef]
3. Thorpe, A.; Harrison, R.M. Sources and properties of nonexhaust particulate matter from road traffic: A review. *Sci. Total Environ.* **2008**, *400*, 270–282. [CrossRef] [PubMed]
4. Rexeis, M.; Hausberger, S. Trend of vehicle emission levels until 2020—Prognosis based on current vehicle measurements and future emission legislation. *Atmos. Environ.* **2009**, *43*, 4689–4698. [CrossRef]
5. Pant, P.; Harrison, R.M. Estimation of the contribution of road traffic emissions to particulate matter concentrations from field measurements: A review. *Atmos. Environ.* **2013**, *77*, 78–97. [CrossRef]
6. Timmers, V.R.J.H.; Achten, P.A.J. Nonexhaust PM emissions from electric vehicles. *Atmos. Environ.* **2016**, *134*, 10–17. [CrossRef]
7. Charron, A.; Polo-Rehn, L.; Besombes, J.L.; Golly, B.; Buisson, C.; Chanut, H.; Marchand, N.; Guillaud, G.; Jaffrezo, J.L. Identification and quantification of particulate tracers of exhaust and nonexhaust vehicle emissions. *Atmos. Chem. Phys.* **2019**, *19*, 5187–5207. [CrossRef]
8. Bayramoğlu Karşı, M.B.; Berberler, E.; Berberler, T.; Aslan, Ö.; Yenisoy-Karakaş, S.; Karakaş, D. Correction and source apportionment of vehicle emission factors obtained from Bolu Mountain Highway Tunnel, Turkey. *Atmos. Pollut. Res.* **2020**, *11*, 2133–2141. [CrossRef]
9. Bukowiecki, N.; Lienemann, P.; Hill, M.; Figi, R.; Richard, A.; Furger, M.; Rickers, K.; Falkenberg, G.; Zhao, Y.; Cliff, S.S.; et al. Real-world emission factors for antimony and other brake wear related trace elements: Size-segregated values for light and heavy duty vehicles. *Environ. Sci. Technol.* **2009**, *43*, 8072–8078. [CrossRef]
10. Demir, T.; Yenisoy-Karakaş, S.; Karakaş, D. PAHs, elemental and organic carbons in a highway tunnel atmosphere and road dust: Discrimination of diesel and gasoline emissions. *Build. Environ.* **2019**, *160*, 106166. [CrossRef]
11. Franco, V.; Kousoulidou, M.; Muntean, M.; Ntziachristos, L.; Hausberger, S.; Dilara, P. Road vehicle emission factors development: A review. *Atmos. Environ.* **2013**, *70*, 84–97. [CrossRef]
12. Gaga, E.O.; Arı, A.; Akyol, N.; Üzmez, Ö.Ö.; Kara, M.; Chow, J.C.; Watson, J.G.; Özel, E.; Döğeroğlu, T.; Odabasi, M. Determination of real-world emission factors of trace metals, EC, OC, BTEX, and semivolatile organic compounds (PAHs, PCBs and PCNs) in a rural tunnel in Bilecik, Turkey. *Sci. Total Environ.* **2018**, *643*, 1285–1296. [CrossRef]
13. Hao, Y.; Deng, S.; Yang, Y.; Song, W.; Tong, H.; Qiu, Z. Chemical composition of particulate matter from traffic emissions in a road tunnel in Xi'an, China. *Aerosol Air Qual. Res.* **2019**, *19*, 234–246. [CrossRef]
14. Jamriska, M.; Morawska, L.; Thomas, S.; He, C. Diesel bus emissions measured in a tunnel study. *Environ. Sci. Technol.* **2004**, *38*, 6701–6709. [CrossRef]
15. Kristensson, A.; Johansson, C.; Westerholm, R.; Swietlicki, E.; Gidhagen, L.; Wideqvist, U.; Vesely, V. Real-world traffic emission factors of gases and particles measured in a road tunnel in Stockholm, Sweden. *Atmos. Environ.* **2004**, *38*, 657–673. [CrossRef]
16. Nogueira, T.; de Souza, K.F.; Fornaro, A.; de Fatima Andrade, M.; de Carvalho, L.R.F. On-road emissions of carbonyls from vehicles powered by biofuel blends in traffic tunnels in the Metropolitan Area of Sao Paulo, Brazil. *Atmos. Environ.* **2015**, *108*, 88–97. [CrossRef]
17. Amato, F.; Pandolfi, M.; Escrig, A.; Querol, X.; Alastuey, A.; Pey, J.; Perez, N.; Hopke, P.K. Quantifying road dust resuspension in urban environment by Multilinear Engine: A comparison with PMF2. *Atmos. Environ.* **2009**, *43*, 2770–2780. [CrossRef]
18. Demir, T.; Karakaş, D.; Yenisoy-Karakaş, S. Source identification of exhaust and nonexhaust traffic emissions through the elemental carbon fractions and Positive Matrix Factorization method. *Environ. Res.* **2022**, *204*, 112399. [CrossRef] [PubMed]
19. Schauer, J.J.; Lough, G.C.; Shafer, M.M.; Christensen, W.F.; Arndt, M.F.; De Minter, J.T.; Park, J.S. Characterization of metals emitted from motor vehicles. *Res. Rep.* **2006**, *133*, 1–76.
20. Sjögren, M.; Li, H.; Rannug, U.; Westerholm, R. Multivariate analysis of exhaust emissions from heavy-duty diesel fuels. *Environ. Sci. Technol.* **1996**, *30*, 38–49. [CrossRef]
21. Cheng, Y.S.; Yamada, Y.; Yeh, H.C.; Swift, D.L. Diffusional deposition of ultrafine aerosols in a human nasal cast. *J. Aerosol Sci.* **1988**, *19*, 741–751. [CrossRef]
22. Thurston, G.D.; Spengler, J.D. A quantitative assessment of source contributions to inhalable particulate matter pollution in metropolitan Boston. *Atmos. Environ.* **1985**, *19*, 9–25. [CrossRef]
23. Pulles, T.; Heslinga, D. *The Art of Emission Inventorying*; TNO: Hague, The Netherlands, 2007. [CrossRef]
24. Smits, M.; Vanpachtenbeke, F.; Horemans, B.; de Wael, K.; Hauchecorne, B.; van Langenhove, H.; Demeestere, K.; Lenaerts, S. Effect of operating and sampling conditions on the exhaust gas composition of small-scale power generators. *PLoS ONE* **2012**, *7*, e32825. [CrossRef] [PubMed]
25. Wang, Y.F.; Huang, K.L.; Li, C.T.; Mi, H.H.; Luo, J.H.; Tsai, P.J. Emissions of fuel metals content from a diesel vehicle engine. *Atmos. Environ.* **2003**, *37*, 4637–4643. [CrossRef]
26. Weber, S.; Hoffmann, P.; Ensling, J.; Dedic, A.N.; Weinbruch, S.; Miehe, G.; Gutlich, P.; Ortner, H.M. Characterization of iron compounds from urban and rural aerosol sources. *J. Aerosol. Sci.* **2000**, *31*, 987–997. [CrossRef]

27. Cheung, K.L.; Ntziachristos, L.; Tzamkiozis, T.; Schauer, J.J.; Samaras, Z.; Moore, K.F.; Sioutas, C. Emissions of Particulate Trace Elements, Metals and Organic Species from Gasoline, Diesel, and Biodiesel Passenger Vehicles and Their Relation to Oxidative Potential. *Aerosol. Sci. Technol.* **2010**, *44*, 500–513. [CrossRef]
28. McKenzie, C.H.L.; Godwin, A.A.; Morawska, L.; Zoran, D.; Ristovski, E.; Rohan, J.; Kokot, S. A comparative study of the elemental composition of the exhaust emissions of cars powered by liquefied petroleum gas and unleaded petrol. *Atmos. Environ.* **2006**, *40*, 3111–3122. [CrossRef]
29. Amato, F.; Pandolfi, M.; Moreno, T.; Furger, M.; Pey, J.; Alastuey, A.; Bukowiecki, N.; Prevot AS, H.; Baltensperger, U.; Querol, X. Sources and variability of inhalable road dust particles in three European cities. *Atmos. Environ.* **2011**, *45*, 6777–6787. [CrossRef]
30. Wang, C.; Chang, C.; Tsai, S.; Chiang, H. Characteristics of Road Dust from Different Sampling Sites in Northern Taiwan. *J. Air Waste Manag. Assoc.* **2005**, *55*, 1236–1244. [CrossRef]
31. Corbin, J.; Mensah, A.A.; Pieber, S.M.; Orasche, J.; Michalke, B.; Zanatta, M.; Czech, H.; Massabò, D.; Buatier de Mongeot, F.; Mennucci, C.; et al. Trace metals in soot and PM2.5 from heavy-fuel-oil combustion in a marine engine. *Environ. Sci. Technol.* **2018**, *52*, 6714–6722. [CrossRef]
32. Gietl, J.K.; Lawrence, R.; Thorpe, A.J.; Harrison, R.M. Identification of brake wear particles and derivation of a quantitative tracer for brake dust at a major road. *Atmos. Environ.* **2010**, *44*, 141–146. [CrossRef]
33. Handler, M.; Puls, C.; Zbiral, J.; Marr, I.; Puxbaum, H.; Limbeck, A. Size and composition of particulate emissions from motor vehicles in the Kaisermühlen-Tunnel, Vienna. *Atmos. Environ.* **2008**, *42*, 2173–2186. [CrossRef]
34. Lawrence, S.; Sokhi, R.; Ravindra, K.; Mao, H.; Prain, H.D.; Bull, I.D. Source apportionment of traffic emissions of particulate matter using tunnel measurements. *Atmos. Environ.* **2013**, *77*, 548–557. [CrossRef]
35. Pio, C.; Mirante, F.; Oliveira, C.; Matos, M.; Caseiro, A.; Oliveira, C.; Querol, X.; Alves, C.; Martins, N.; Cerqueira, M.; et al. Size-segregated chemical composition of aerosol emissions in an urban road tunnel in Portugal. *Atmos. Environ.* **2013**, *71*, 15–25. [CrossRef]
36. Sternbeck, J.; Sjödin, Å.; Andréasson, K. Metal emissions from road traffic and the influence of resuspension—Results from two tunnel studies. *Atmos. Environ.* **2002**, *36*, 4735–4744. [CrossRef]
37. Harrison, R.M.; Jones, A.M.; Gietl, J.; Yin, J.; Green, D.C. Estimation of the contributions of brake dust, tire wear, and resuspension to nonexhaust traffic particles derived from atmospheric measurements. *Environ. Sci. Technol.* **2012**, *46*, 6523–6529. [CrossRef]
38. Pant, P.; Shi, Z.; Pope, F.D.; Harrison, R.M. Characterization of traffic-related particulate matter emissions in a road tunnel in Birmingham, UK: Trace metals and organic molecular markers. *Aerosol. Air Qual. Res.* **2017**, *17*, 117–130. [CrossRef]
39. Sanders, P.G.; Xu, N.; Dalka, T.M.; Maricq, M.M. Airborne brake wear debris: Size distributions, composition, and a comparison of dynamometer and vehicle tests. *Environ. Sci. Technol.* **2003**, *37*, 4060–4069. [CrossRef] [PubMed]
40. Marr, I.L.; Kluge, P.; Main, L.; Margerin, V.; Lescop, C. Digests or extracts? Some interesting but conflicting results for three widely differing polluted sediment samples. *Mikrochim. Acta* **1995**, *119*, 219–232. [CrossRef]
41. Hoekman, S.K.; Leland, A. Literature Review on the Effects of Organometallic Fuel Additives in Gasoline and Diesel Fuels. *SAE Int. J. Fuels Lubr.* **2018**, *11*, 105–124. [CrossRef]
42. Bayramoğlu Karşı, M.B.; Berberler, E.; Karakaş, D. Polycyclic aromatic hydrocarbon and ionic compositions of atmospheric bulk deposition samples at a national park under the influence of intense barbecue smoke. *Int. J. Environ. Anal. Chem.* **2019**, *99*, 428–443. [CrossRef]
43. Yang, H.H.; Dhital, N.B.; Wang, L.C.; Hsieh, Y.S.; Lee, K.T.; Hsu, Y.T.; Huang, S.C. Chemical characterization of fine particulate matter in gasoline and diesel vehicle exhaust. *Aerosol. Air Qual. Res.* **2019**, *19*, 1439–1449. [CrossRef]
44. Galvão, E.S.; D'Azeredo Orlando, M.T.; Santos, J.M.; Lima, A.T. Uncommon chemical species in PM2.5 and PM10 and its potential use as industrial and vehicular markers for source apportionment studies. *Chemosphere* **2020**, *240*, 124953. [CrossRef] [PubMed]
45. Fabretti, J.F.; Sauret, N.; Gal, J.F.; Maria, P.C.; Scharer, U. Elemental characterization and source identification of PM2.5 using Positive Matrix Factorization: The Malraux road tunnel, Nice, France. *Atmos. Res.* **2009**, *94*, 320–329. [CrossRef]
46. Lin, Y.C.; Tsai, C.J.; Wu, Y.C.; Zhang, R.; Chi, K.H.; Huang, Y.T.; Lin, S.H.; Hsu, S.C. Characteristics of trace metals in traffic-derived particles in Hsuehshan Tunnel, Taiwan: Size distribution, potential source, and fingerprinting metal ratio. *Atmos. Chem. Phys.* **2015**, *15*, 4117–4130. [CrossRef]
47. Kurre, S.K.; Pandey, S.; Garg, R.; Saxena, M. Condition monitoring of a diesel engine fueled with a blend of diesel, biodiesel, and butanol using engine oil analysis. *Biofuels* **2015**, *6*, 223–231. [CrossRef]
48. USEPA. Emission Factor Documentation for AP-42, Section 13.2.1 Paved Roads. 2011. Available online: https://www.epa.gov/sites/default/files/2020-10/documents/emission_factor_documentation_for_ap-2_section_13.2.1_paved_roads_.pdf (accessed on 26 September 2022).
49. Han, S.; Jung, Y.W. A study of the characteristic of silt loading on the paved roads in the Seoul metropolitan area using a mobile monitoring system. *J. Air. Waste Manag. Assoc.* **2012**, *62*, 846–862. [CrossRef]
50. Çevik, F.; Göksu, M.Z.L.; Derici, O.B.; Findik, Ö. An assessment of metal pollution in surface sediments of Seyhan dam by using enrichment factor, geoaccumulation index and statistical analyses. *Environ. Monit. Assess.* **2009**, *152*, 309–317. [CrossRef]
51. Alves, C.A.; Evtyugina, M.; Vicente, A.M.P.; Vicente, E.D.; Nunes, T.V.; Silva, P.M.A.; Duarte, M.A.C.; Pio, C.A.; Amato, F.; Querol, X. Chemical profiling of PM10 from urban road dust. *Sci. Total Environ.* **2018**, *634*, 41–51. [CrossRef]
52. Barbieri, M. The Importance of Enrichment Factor (EF) and Geoaccumulation Index (Igeo) to Evaluate the Soil Contamination. *J. Geol. Geophys.* **2016**, *5*, 1–4. [CrossRef]

53. Kryłów, M.; Generowicz, A. Impact of street sweeping and washing on the pm10 and PM2.5 concentrations in cracow (Poland). *Rocz. Ochr. Sr.* **2019**, *21*, 691–711.
54. Birch, M.E.; Cary, R.A. Elemental Carbon-Based Method for Monitoring Occupational Exposures to Particulate Diesel Exhaust. *Aerosol. Sci. Technol.* **1996**, *25*, 221–241. [CrossRef]
55. Karanasiou, A.; Diapouli, E.; Cavalli, F.; Eleftheriadis, K.; Viana, M.; Alastuey, A.; Querol, X.; Reche, C. On the quantification of atmospheric carbonate carbon by thermal/optical analysis protocols. *Atmos. Meas. Tech.* **2011**, *4*, 2409–2419. [CrossRef]